Photochemical & Photobiological Sciences
https://doi.org/10.1007/s43630-025-00842-4

RESEARCH

Hydrothermally synthesized silver-decorated propolis quantum dots: a dual-action antibacterial and antioxidant nanocomposite

Ruba Jebril[1] · Seyda Albayrak[1] · Hayrunnisa Nadaroglu[2,3] · Ahmet Adiguzel[1]

Received: 29 August 2025 / Accepted: 30 November 2025
© The Author(s) 2026

Abstract
Propolis carbon quantum dots (PCQDs) and silver nanoparticles (AgNPs) were hydrothermally synthesized. The PCQD@Ag nanocomposite was formed by reducing silver nitrate ($AgNO_3$) with sodium citrate. PCQDs and AgNPs were characterized by UV spectroscopy, photoluminescence (PL) spectroscopy, Fourier Transform Infrared Spectroscopy (FTIR), and Transmission Electron Microscopy (TEM). In addition, X-ray diffraction (XRD) was also performed on AgNPs. The antioxidant activities of AgNPs, PCQDs, and PCQDs@AgNPs were also studied. Furthermore, their antibacterial activities were investigated under fluorescent light by comparing bacterial strains isolated from periodontal abscesses. It was observed that PCQDs and AgNPs had dimensions of 8–10 nm and 20–35 nm, respectively, and PCQDs exhibited a strong fluorescence peak around 380 nm. PCQDs were found to be a potent photosensitizer. PCQDs, AgNPs, and PCQD@AgNPs exhibited antibacterial activity against periodontal abscess-causing bacteria and demonstrated strong antioxidant activity.

Keywords Propolis carbon quantum dots · Silver nanoparticles · Antibacterial activity · Antioxidant activity · Photodynamic therapy

1 Introduction

Periodontal abscesses are considered serious complications in dentistry. This condition occurs when pus accumulates in the gum wall, and if left untreated, it can cause the infection to spread throughout the body. Penicillin, amoxicillin, metronidazole, tetracycline, clindamycin, doxycycline, and erythromycin are recommended for the treatment of periodontal abscesses. However, incorrect and excessive use of antibiotics during the treatment process leads to an increase in antibiotic resistance, which causes significant health problems, especially in developing countries. In this context, the need for alternative treatment methods against antibiotic-resistant pathogens is increasing [1–11].

Nanoparticles are an effective alternative to antibiotics. Silver nanoparticles (AgNPs), in particular, are promising candidates as they were used as antimicrobial agents in the treatment of burns and open wounds before the development of antibiotic therapy. Thanks to their high surface area and strong antibacterial properties, they offer a promising option for treating bacterial infections. AgNPs can effectively kill microorganisms by damaging bacterial cellular structures [12–15]. Photodynamic therapy (PDT) has also been developed with advances in nanoparticle research, and this approach has been shown to exhibit antimicrobial properties. PDT uses light-activated photosensitizers to produce reactive oxygen species, which then kill microorganisms. The effectiveness of PDT depends on the appropriate photosensitizer, light source, and oxygen availability [16, 17]. Carbon quantum dots (CQDs) are tiny carbon-based

✉ Ahmet Adiguzel
adiguzel@atauni.edu.tr

Ruba Jebril
rubamaher810@gmail.com

Seyda Albayrak
aseyda@atauni.edu.tr

Hayrunnisa Nadaroglu
hnisa25@atauni.edu.tr

[1] Department of Molecular Biology and GeneticsFaculty of Science, Ataturk University, Erzurum 25240, Turkey

[2] Department of Food Technology, Vocational College of Technical SciencesAtaturk University, Erzurum 25240, Turkey

[3] Department of Nano-Science and Nano-Engineering, Institute of ScienceAtaturk University, Erzurum 25240, Turkey

Published online: 20 January 2026

nanoparticles with surface passivation. They are categorized as zero-dimensional (OD) nanostructures, with sizes typically less than 10 nm, making them among the smallest nanomaterials. They have various features, including easy synthesis methods, low toxicity, high biocompatibility, and suitability for surface modification. These unique properties have made CQDs promising candidates for a wide range of biomedical applications, including antibacterial, cancer, drug delivery, bioimaging, antiviral, and wound-healing applications. Nanomaterials such as CQDs have emerged as a promising option for photodynamic therapy. Natural compounds are also used in the production of CQDs [18–23]. When it comes to natural compounds, propolis comes to mind first. Propolis is not limited to antibacterial activity; it also has antiviral, antiprotozoal, antifungal, antiparasitic, antioxidant, antitumor, and anti-inflammatory activities. The chemical composition of propolis is quite complex and consists mainly of 50% balsam and resin, 30% wax, 10% essential oils, 10% pollen, and 5% other organic compounds, including sugars, amino acids, vitamins (B complex, C, and E), and minerals. Propolis content varies depending on the plant diversity of the region where it is collected, climatic conditions, and the genetic structure of the bee [24–28].

All this information indicates that a periodontal abscess needs urgent treatment. Given the global crisis of multidrug resistance, there is also a need for a natural alternative. PDT is considered a promising and suitable antimicrobial option. Existing studies focus on isolating and characterizing bacteria that cause dental abscesses. However, research into developing alternatives to antibiotics and mouthwashes is limited. To our knowledge, no studies have yet explored the antibacterial activity of propolis carbon quantum dots (PCQDs) decorated with silver nanoparticles (AgNPs) as photosensitizers against pathogens causing periodontal abscesses. In this study, PCQDs were produced from propolis sourced from local suppliers, and AgNPs were synthesized using sodium citrate. The resulting PCQDs were characterized. Their effectiveness was demonstrated by comparing them with nearly all the antibiotics currently available on the market, as well as through antioxidant and antibacterial testing.

2 Materials and methods

2.1 Propolis

The propolis sample was collected from Erzurum, Türkiye, in the winter of 2022 and stored at -20 °C for later use.

2.2 Determination of the chemical composition of the propolis sample

The chemical composition of the propolis was determined using a Gas Chromatography-Mass Spectrometry (GC-MS) Shimadzu QP2010 ULTRA. The analysis was carried out at the Eastern Anatolia High Technology Application and Research Center (DAYTAM) of Atatürk University.

2.3 Synthesis of silver nanoparticles and propolis carbon quantum Dot

Propolis quantum dots (PCQDs) were synthesized hydrothermally according to the method described by [29]. Briefly, 0.1 g of propolis and 0.65 g of Sodium-Citrate were dissolved in 80 mL of deionized distilled water and placed in an autoclave at 200 °C for 8 h. After autoclaving, the suspension was centrifuged at 15,000 rpm for 30 min and filtered using a 0.22 µm filter paper.

For the synthesis of AgNPs, 0.65 g of Sodium Citrate was added to a 1 mM AgNO3 solution, which was then dissolved in 80 mL deionized distilled water. After adding 1 mL of NH3 solution, the sample was placed in the autoclave at 200 °C for 8 h. After autoclaving, the suspension was centrifuged at 15,000 rpm for 30 min. The obtained AgNPs were first washed with distilled water, then with ethyl alcohol, and finally dried in an oven at 60 °C under vacuum. The samples were stored at 4 °C until use [30]. The PCQD@Ag modified structure was formed by reducing silver nitrate ($AgNO_3$) with sodium citrate.

2.4 Characterization studies

Characterization of PCQDs and AgNPs was carried out at the Eastern Anatolia High Technology Application and Research Center (DAYTAM) of Atatürk University. The morphological structures of CQDs and AgNPs were examined using Transmission Electron Microscopy (TEM) on a Hitachi HT-7700. At the same time, the crystallinity and phase purity of PCQDs and AgNPs were analyzed by X-ray diffraction (XRD) analysis using the PANalytical Empyrean instrument. A Fourier Transform Infrared Spectrophotometer (Bruker VERTEX 70v FTIR) was used to determine the functional groups on the surfaces of PCQDs and AgNPs. UV-Vis spectroscopy (Shimadzu UV-3600 Plus) and photoluminescence (PL) spectra were obtained for the optical characterization of PCQDs.

2.5 Bacterial strains

In this study, 14 bacterial strains isolated from periodontal abscesses (Table 1), as well as standard strains of

Table 1 Bacterial strains isolated from periodontal abscess

Code	Bacterial strain	Acceptance number
K1	*Staphylococcus haemolyticus*	MF578766
K5	*Staphylococcus equorum*	MF578770
K16	*Streptococcus massiliensis*	MF578780
K17	*Streptococcus gordonii*	MF578781
K18	*Streptococcus anginosus*	MF578782
K38	*Streptococcus oralis*	MF578798
K39	*Streptococcus cristatus*	MF578799
K41	*Streptococcus sinensis*	MF578822
K44	*Streptococcus gordonii*	MF578802
K45	*Streptococcus constellatus*	MF578803
K47	*Streptococcus sanguinis*	MF578804
K50	*Actinomyces oris*	MF578807
K51	*Streptococcus mutans*	MF578808
K57	*Streptococcus anginosus*	MF578814

Staphylococcus epidermidis ATCC 12,228, *Streptococcus pyogenes* ATCC 19,615, *Staphylococcus aureus* ATCC 25,323, *Klebsiella pneumoniae* ATCC 13,883, *Pseudomonas aeruginosa* ATCC 27,853, *Escherichia coli* O157:H7 ATCC 43,894, and *Bacillus cereus* ATCC 11,778 were used.

2.6 Determination of antibacterial activity

The disc diffusion method was used to test the antibacterial activity of modified propolis quantum dots (PCQDs@AgNPs) and silver nanoparticles (AgNPs). All bacterial strains were inoculated on TSA medium using the streaking method and incubated at 37 °C for 48 h. The purity of the isolates was checked on the surface of the Petri dishes and under a microscope. A single colony was transferred to 50 mL of TSB, autoclaved, and incubated at 37 °C for 48 h. Samples of the developing cultures were taken, inoculated into tubes containing 0.9% saline, and adjusted to 0.5 McFarland. The bacterial suspension was spread on agar using a sterile cotton swab and allowed to stand for a few minutes. Blank discs were then placed, and the tested material was applied. Chlorhexidine and water were used as positive and negative controls, respectively. The plates were incubated at 37 °C for 24 h under visible light, and the zone of inhibition was measured in millimeters (mm) after the incubation [31].

2.7 Antibiotic susceptibility testing

Antibiotic susceptibility testing was performed for each isolate on separate Petri dishes as.

a reference to compare the antibacterial activity of the tested material. The antibiotics used were kanamycin, gentamicin, streptomycin, netilmicin, sulbactam, ampicillin, amoxicillin, vancomycin, ofloxacin, chloramphenicol, cefoperazone, sulfamethoxazole, and ciprofloxacin. As in the antibacterial activity test, the strains were revived from stock using TSA medium and incubated in TSB medium. The bacterial suspension was then adjusted to 0.5 McFarland in tubes containing 0.9% saline. The bacterial suspension was spread on agar using sterile cotton swabs, left in a sterile cabinet for a few minutes, and then antibiotic disks were applied. The plates were incubated at 37 °C for 24 h, and the zone of inhibition was measured in millimeters (mm) after the incubation.

2.8 Antioxidant test

The radical scavenging abilities of the synthesized AgNPs, PCQDs, and PCQDs@AgNPs were evaluated using 1,1-diphenyl-2-picrylhydrazyl (DPPH) and the ferric ion (Fe^{3+}) reducing antioxidant power Assay (FRAP).

2.8.1 1,1-Diphenyl-2-picrylhydrazyl (DPPH)

The DPPH radical-scavenging activity of AgNPs, PCQDs, and PCQDs@AgNPs was investigated using the BOLIS method. Using butylated hydroxyanisole (BHA) and α-tocopherol as standards, the results were expressed as percent reduction according to the following formula:

$$DPPH\ scavenging\ effect\ (\%) = \frac{A\ control - A\ sample}{A\ control} \times 100$$

To 100 µL of DPPH solution (0.1%), 30 and 50 µg of AgNPs, PCQDs, and PCQDs@AgNPs were added, and the mixture was incubated at room temperature for 30 min. The absorbance (A) was then measured at 517 nm using a spectrophotometer. This step was repeated three times to ensure the reliability and validity of the results [32, 33].

2.8.2 Ferric ions (Fe^{3+}) reducing antioxidant power assay (FRAP)

To determine the reducing power of AgNPs, PCQDs, and PCQDs@AgNPs, 30 and 50 µg/mL concentrations of the tested materials were mixed with sodium phosphate buffer (2.5 mL, 0.2 M, pH 6.6) and potassium ferricyanide (2.5 mL, 1%) in 1 mL of distilled water. The resulting mixture was incubated at 50 °C for 20 min, and 10% TCA was then added. The supernatant (2.5 mL) was collected, and equal volumes of distilled water and 0.5 mL of 0.1% ferric chloride were added. The absorbance was then measured at 700 nm using a spectrophotometer. The higher absorbance value indicates an increased reducing power [34, 35].

Table 2 Chemical composition of propolis

Peak list				
m/z	z	Abund	Name	Formula
79.01867		2272.35	Fluoroacetate	C2 H3 F O2
209.04161		2399.04	Endothall	C8 H10 O5
269.07847	1	6216.23	DHAP (6:0)	C9 H17 O7 P
270.08176	1	1036.16		C9 H17 O7 P
271.05809	1	944.38		C9 H17 O7 P
323.25622	1	19010.37	14-hydroxy stearic acid	C18 H36 O3
324.25957	1	3664.32		C18 H36 O3
325.26907	1	1386.66		C18 H36 O3
393.07825		4002.97	Ferulic acid 4-O-glucuronide	C16 H18 O10
539.50335	1	5393.55	12-PAHSA	C34 H66 O4
540.50679	1	1899.58		C34 H66 O4
561.48539	1	4464.08	12-PAHSA	C34 H66 O4
562.48867	1	1610.39		C34 H66 O4
673.6117	1	7692.57	2 S, 3R-didecanoyl-docosane-2,3-diol	C42 H82 O4
815.71237	1	2936.91	TG(13:0/16:0/20:3(8Z,11Z,14Z)) [iso6]	C52 H94 O6

3 Result and discussion

3.1 GC-MS analysis of propolis sample

The chemical composition of propolis is highly complex and varies depending on the plant diversity in the region where it is collected, the climatic conditions, and the genetic background of the bee species. Since propolis is mainly composed of phytochemicals, and its biological activities depend on these compounds, investigating its chemical profile is of great importance [36–38].

In a study by [39], propolis samples from the Kashmir region were analyzed using GC–MS, and the most dominant compounds identified were alpha-D-mannopyranoside, methyl, cyclic 2,3:4,6-bis-ethyl boronate (21.17%), hexamethanic acid methyl ester (9.91%), and bacteriochlorophyll c-stearyl (4.41%). Another study by [40] on Brazilian (Paraná) propolis reported the presence of succinic, palmitic, oleic, retinoic, and p-coumaric acids.

In the present study, propolis samples from Erzurum, Türkiye, were analyzed. GC–MS analysis revealed the presence of fluoroacetate, endothall, DHAP (6:0), 14-hydroxystearic acid, ferulic acid 4-O-glucuronide, 12-PAHSA, 2,3-diol TG (13:0/16:0/20:3(8Z,11Z,14Z)) [iso6], and 2 S,3R-dodecanol-docosane (Table 2).

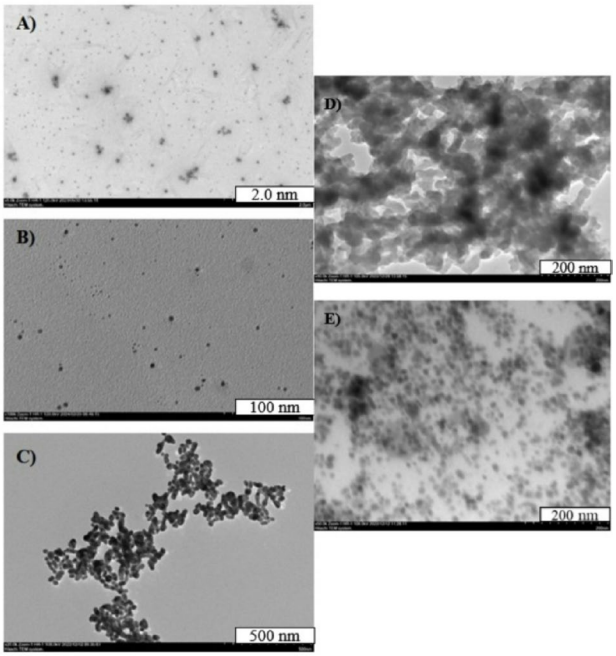


Fig. 1 TEM images of PCQD (**A** and **D**) and AgNPs (**B**, **C**, and **E**)

3.2 Characterization studies results

3.2.1 TEM results

In this study, TEM images were used to examine the morphological characteristics and surface features of PCQDs and AgNPs. The TEM analysis of PCQDs revealed that, although slight aggregation was observed in some areas, the particles were predominantly homogeneous, exhibiting sizes ranging from **8 to 10 nm** (Fig. 1A). Similarly [29], reported hydrothermally synthesized propolis CQDs with particle sizes of **4–6 nm**, while [41] documented propolis-derived CQDs measuring **1–2 nm**. These findings align with

the literature, which indicates that carbon quantum dots typically have diameters below 10 nm, although their exact size can vary with synthesis conditions.

TEM images of AgNPs (Fig. 1B and C) revealed particles with an **almost spherical morphology**, a **smooth surface**, and an average size range of **20–35 nm**. The AgNPs synthesized in this study closely resemble those reported in previous research [42, 43], demonstrating similar morphological characteristics and size distributions.

3.2.2 Optical properties of PCQD and AgNPs

Absorption, excitation, and fluorescence measurements were performed to characterize the PCQDs optically. The absorption behavior of the synthesized PCQDs was determined by UV-vis spectroscopy, and the emission behavior was determined by PL spectra (Fig. 2A and B). The dark brown PCQDs showed distinct peaks at the maximum excitation and emission wavelengths, corresponding to the bright blue fluorescence observed when the solution was illuminated with a UV lamp at 420 nm. When the absorbance of PCQDs was scanned in the range of 200–700 nm, a maximum peak at 280 nm was observed (Fig. 2A). This peak is associated with the typical $\pi \rightarrow \pi^*$ transition band of aromatic (C=C) sp2 hybrid orbitals. This indicates the formation of CQDs.

However, in Fig. 2B, the fluorescence spectra of PCQDs were recorded over an excitation wavelength range of 340–410 nm. Emission maxima were observed between approximately 430 and 460 nm, and both the emission intensity and peak varied nonmonotonically with excitation wavelength. Specifically, the fluorescence intensity initially increased and then decreased with increasing excitation wavelength, and a slight redshift of the emission peak was observed. This excitation-dependent behavior is due to differences in surface properties and particle size distributions within the PCQDs.

Although the strongest absorption occurs at 280 nm, excitation wavelengths above 340 nm were chosen because the UV region below 300 nm can cause internal filter effects and reabsorption, and visible excitation allows for more precise observation of fluorescence behavior, which is essential for sensing and biological imaging applications.

Additionally, to clarify the excitation-induced emission behavior, the peak emission wavelength and fluorescence intensity were plotted as a function of excitation wavelength (Fig. 2B). This plot quantitatively shows a slight redshift and a non-monotonic intensity change. The results are consistent with the literature [44–46].

An absorption peak was observed at approximately 420 nm for AgNPs, as shown in Fig. 2A. This indicates that the surface plasmon of the AgNPs was excited, confirming the formation of AgNPs [47–49]. Using the data from Fig. 2, the maximum emission wavelength of PCQDs increases with excitation wavelength, indicating an excitation-dependent redshift. Additionally, the maximum fluorescence intensity varies with excitation and peaks at 380 nm at

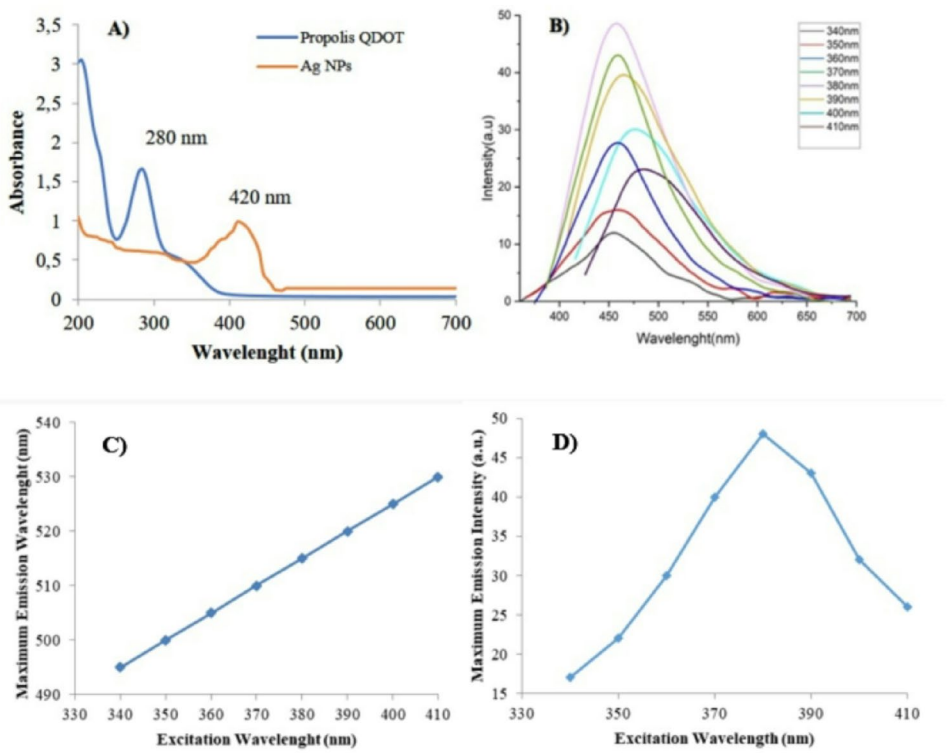


Fig. 2 **A** Absorption wavelength of PCQDs and AgNPs, **B** Fluorescence measurements of PCQDs at the excitation wavelength, **C** Maximum emission wavelength as a function of excitation wavelength, showing red-shift, **D** Maximum fluorescence intensity as a function of excitation wavelength

the optimal excitation wavelength, demonstrating efficient emission under certain excitation conditions [50].

3.2.3 FTIR and XRD analysis of PCQD and AgNPs

Fourier Transform Infrared (FTIR) Spectroscopy analysis was performed to identify the functional groups present on the surfaces of PCQDs and AgNPs. The FTIR spectrum of AgNPs is shown in Fig. 3. The peak at 3608 cm^{-1} of the synthesized AgNPs corresponds to the stretching vibration of a hydroxyl group (-OH). The peaks at 2451–2042 cm-1 may be due to the vibrations of the C-C bonds, while the peak at 1502 cm-1 is associated with C=O and amine (N-H) groups. Furthermore, the peaks at 1161–875 cm-1 correspond to C-O groups, while the peak at 568 cm-1 is attributed to C-H bending vibrations [50, 51].

Figure 3 shows the FTIR spectrum of the CQDs. Three absorbance peaks were observed: the broad peak at 3330 cm-1 corresponds to -OH stretching vibrations, the weak peak at 1658 cm-1 corresponds to C=O or C=C groups, and the weak peak at 1056 cm-1 is assigned to C-O stretching vibrations. The results obtained in this study are consistent with previous reports [52–55].

X-ray diffraction (XRD) analysis is a rapid, efficient technique commonly used to identify the crystal structures of nanoscale materials and to distinguish between amorphous and crystalline forms. Owing to its accuracy, it is considered one of the most reliable methods for this purpose. The XRD pattern of the synthesized AgNPs exhibited four prominent peaks located at 2Θ values of 38.5◦, 45.6◦, 64.5◦, and 78◦, corresponding to the (111), (200), (220), and (311) planes of face-centered cubic (fcc) silver, confirming their crystalline nature (Fig. 3B) [56, 57].

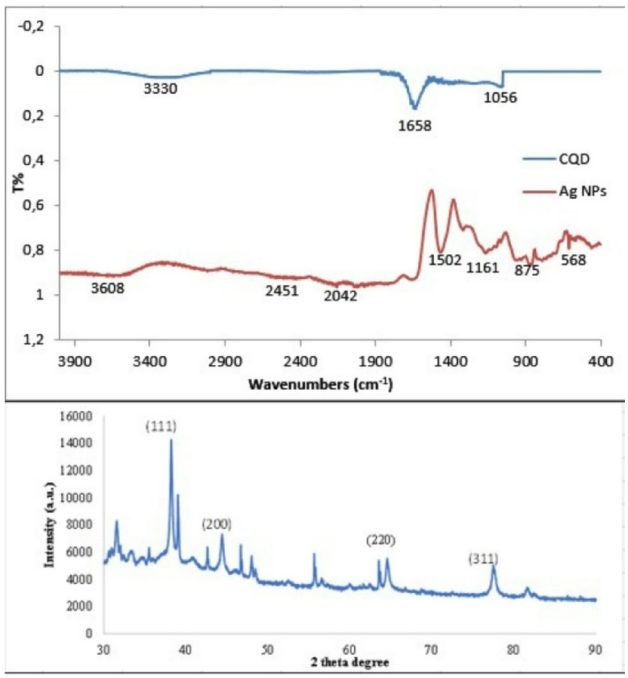


Fig. 3 FTIR spectrum of AgNPs and CQDs (**A**), and XRD analysis of AgNPs (**B**)

3.3 Antibacterial activity of PCQDs/AgNPs and AgNPs

Propolis, a natural compound produced by honey bees, is well known for its antibacterial properties against both Gram-negative and Gram-positive bacteria [26]. The antimicrobial activity of propolis has been investigated against many pathogens, including oral pathogens, and it has been found effective against those causing periodontal abscesses [58, 59]. To enhance the activity of this substance, already known for its high antimicrobial potential, PCQDs were synthesized and conjugated to AgNPs, which also possess strong antimicrobial activity. The remarkable antibacterial activity of PCQDs@AgNPs and AgNPs against isolated strains is shown in Table 3, and selected inhibition zones are shown in Fig. 4. It was found that both Gram-positive and Gram-negative strains were highly susceptible to PCQDs@AgNPs and AgNPs, with inhibition zones ranging from 8 mm to 20 mm.

Although PCQD@AgNPs exhibited antibacterial activity against all tested bacterial strains, some were resistant to conventional antibiotics. At the same time, as presented in Table 3, the antibacterial activity of PCQDs was comparable to that of traditional antibiotics. In the study, the inhibition zone observed with Gram-negative bacteria sometimes exceeded that observed with Gram-positive bacteria, and vice versa. Therefore, it is challenging to establish a precise correlation between PCQD@AgNPs and their activity against Gram-positive or Gram-negative bacteria, or to determine which group is more susceptible. In the study conducted by [22], CQDs@AgNPs were synthesized hydrothermally, with CQDs functionalized (doped) with nitrogen and sulfur. Their antibacterial activity was tested against *S. aureus*, *E. coli*, and MARS (Methicillin-resistant *Staphylococcus aureus*), demonstrating effectiveness against these strains and showing stronger activity against Gram-positive than Gram-negative bacteria. In the study by [60], hydrothermally produced CQDs@AgNPs exhibited antibacterial activity against *E. coli*. NK Tenkayala et al.. (2024) tested CQDs@AgNPs against *E. coli*, *P. aeruginosa*, *S. aureus*, and *B. cereus*, finding activity against all four bacterial strains. CQDs@AgNPs produced by [61] displayed stronger antibacterial effects against *E. coli* (Gram-negative) than *S. aureus* (Gram-positive). Similarly [62], reported that CQDs exhibited strong antibacterial activity against *E. coli* and *S. aureus* and found that CQDs showed strong antibacterial

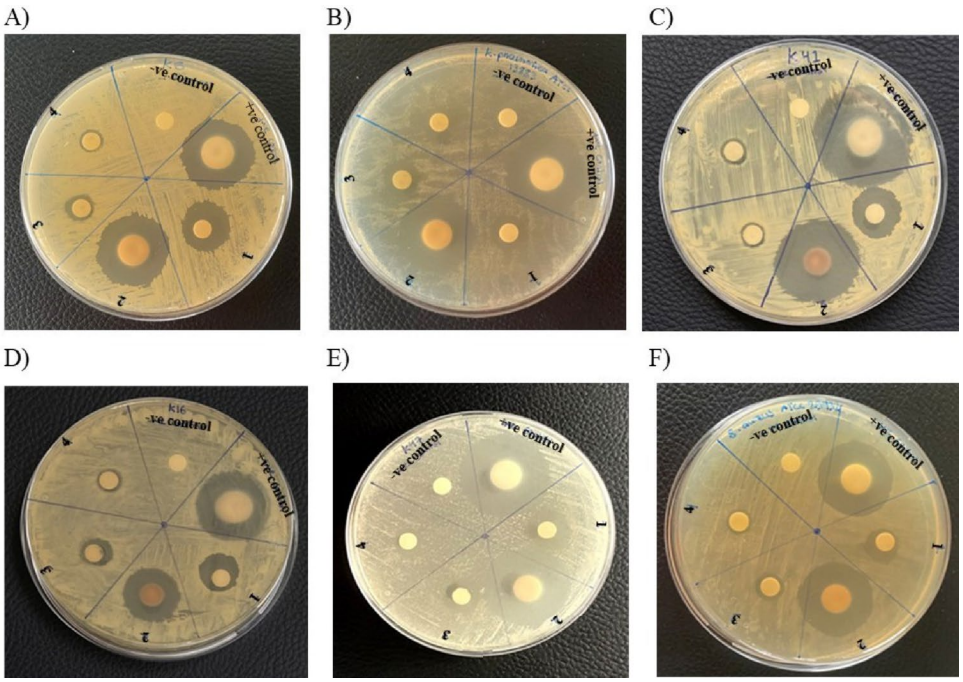


Fig. 4 Antibacterial activity of PCQDs and AgNPs. **A***Staphylococcus equorum*, **B***Klebsiella pneumoniae* ATCC 13883, **C***Streptococcus sinensis*, **D***Streptococcus massiliensis*, **E***Streptococcus sanguinis*, **F***Escherichia coli* O157: H7 ATCC 43894. Antibacterial activity was assessed by disc diffusion. CHX and water: The Positive and the negative control, respectively. (1) PCQD, (2) PCQD + CHX, (3) PCQD@AgNP, and (4) AgNP

activity against both bacterial strains. These literature findings on CQDs@AgNPs are consistent with our study.

AgNPs damage the cell membrane and increase its permeability by producing active compounds, which bind to bacterial biomolecules and block signal transduction pathways in bacterial cells. Consequently, they exhibit a broad spectrum of antibacterial activity [63]. Several studies have evaluated the antibacterial activity of AgNPs against various bacterial pathogens, including oral pathogens.

For example [64], reported that *S. aureus* was susceptible to AgNPs. A similar study [65] found that *S. epidermidis* and *S. haemolyticus* were susceptible to AgNPs [49]. observed antibacterial activity of AgNPs against *S. aureus*, *P.aeruginosa*, and *E.coli*. In another study [66], *S. mutans* was found to be susceptible to AgNPs [67]. reported that alpha-lipoic acid-capped AgNPs were active against *E. coli*, *P. aeruginosa*, *S. mutans*, and *S. gordonii*. Similarly [68], treated *K. pneumoniae* with AgNPs, and [69] found that AgNPs were bactericidal against *S. mitis*, *S. mutans*, and *S. oralis*. Another study [70] showed the sensitivity of *S. pyogenes* to AgNPs. These studies align with this study's results, indicating that the AgNPs synthesized here exhibit high antibacterial activity.

The CQDs and AgNPs demonstrated broad-spectrum antibacterial activity against both Gram-positive and Gram-negative bacterial strains. The antibacterial effects of CQDs and AgNPs are thought to result from various mechanisms, including disruption of cell membrane structure and interactions with biomolecules in DNA and protein structures [63, 71].

In previous studies, most research focused on using AgNPs, CQDs, or propolis individually against bacteria. However, our study is distinguished by a dual nanocomposite of silver-decorated propolis quantum dots, which demonstrated enhanced efficacy against a wide range of bacterial strains and, in some cases, outperformed certain conventional antibiotics, setting it apart from earlier research and highlighting its potential in biomedical applications.

3.4 Antibiotic sensitivity test

The zones of inhibition (in millimeters) of the tested bacterial strains are presented in Table 3; Fig. 4, and Supplementary material. Most antibiotics were effective against the tested bacteria; however, sulbactam (a beta-lactam) and sulfamethoxazole (a sulfonamide) antibiotics did not produce inhibition zones for most bacterial strains. Exceptions include *E. coli* O157:H7, K38 (*Streptococcus oralis*), K16 (*Streptococcus massiliensis*), K44 (*Streptococcus gordonii*), and K50 (*Actinomyces oris*), which were sensitive to sulbactam, whereas *P. aeruginosa* and K1 (*Staphylococcus haemolyticus*) were sensitive to sulfamethoxazole.

3.5 Antioxidant activity

In biological systems, free radicals are primarily generated from oxygen (reactive oxygen species) and nitrogen (reactive nitrogen species, RNS). The accumulation of these molecules within cells induces oxidative stress, which can contribute to cancer, neurodegenerative diseases, and aging. Antioxidants are compounds that prevent or delay oxidative

Table 3 Antibacterial activity

	Ciprofloxacin	Sulfamethoxazole	Cefoperazone	Chloramphenicol	Ofloxacin	Vancomycin	Amoxicillin	Ampicillin	Sulbactam	Netilmicin	Streptomycin	Gentamicin	Kanamycin	CHX	PCQD	PCQDs@CHX	AgNPs@PCQD	AgNP
B. cereus ATCC 11,778	25 mm	R	29 mm	24 mm	21 mm	17 mm	44 mm	44 mm	R	24 mm	16 mm	22 mm	20 mm	37 mm	16 mm	36 mm	14 mm	12 mm
E. coli 0157:H7 ATCC 43,894	35 mm	R	29 mm	24 mm	34 mm	R	19 mm	14 mm	10 mm	24 mm	19 mm	21 mm	22 mm	26 mm	16 mm	24 mm	14 mm	11 mm
K. pneuminia ATCC 13,883	34 mm	R	23 mm	28 mm	32 mm	R	R	R	R	20 mm	15 mm	17 mm	18 mm	29 mm	15 mm	28 mm	15 mm	14 mm
P. aeruginosa ATCC 27,853	34 mm	27 mm	25 mm	21 mm	27 mm	21 mm	28 mm	26 mm	R	29 mm	22 mm	24 mm	25 mm	24 mm	17 mm	21 mm	14 mm	13 mm
S. aureus ATCC 25,323	19 mm	R	20 mm	19 mm	20 mm	16 mm	39 mm	37 mm	R	21 mm	16 mm	20 mm	21 mm	27 mm	14 mm	27 mm	12 mm	11 mm
S. epiderms ATCC 12,228	26 mm	R	15 mm	14 mm	23 mm	18 mm	R	R	R	24 mm	R	25 mm	21 mm	24 mm	12 mm	24 mm	11 mm	11 mm
S. pyogenes ATCC 19,615	27 mm	R	34 mm	29 mm	21 mm	21 mm	28 mm	26 mm	R	20 mm	19 mm	20 mm	20 mm	29 mm	22 mm	28 mm	14 mm	11 mm
K57	23 mm	R	39 mm	34 mm	19 mm	24 mm	39 mm	34 mm	R	19 mm	14 mm	14 mm	14 mm	26 mm	18 mm	25 mm	11 mm	10 mm
K41	29 mm	R	34 mm	34 mm	25 mm	26 mm	34 mm	34 mm	R	19 mm	19 mm	18 mm	17 mm	44 mm	16 mm	39 mm	16 mm	14 mm
K38	44 mm	R	36 mm	34 mm	29 mm	22 mm	40 mm	39 mm	14 mm	39 mm	29 mm	34 mm	34 mm	33 mm	17 mm	33 mm	16 mm	13 mm
K16	19 mm	R	24 mm	26 mm	22 mm	26 mm	34 mm	32 mm	14 mm	14 mm	12 mm	13 mm	R	25 mm	19 mm	24 mm	13 mm	11 mm
K1	30 mm	15 mm	30 mm	29 mm	24 mm	20 mm	36 mm	34 mm	R	36 mm	29 mm	34 mm	34 mm	27 mm	20 mm	26 mm	13 mm	12 mm
K44	24 mm	R	34 mm	31 mm	19 mm	24 mm	41 mm	34 mm	14 mm	18 mm	18 mm	13 mm	14 mm	35 mm	17 mm	32 mm	12 mm	12 mm
K39	24 mm	R	29 mm	24 mm	24 mm	24 mm	34 mm	24 mm	R	19 mm	20 mm	19 mm	18 mm	38 mm	19 mm	38 mm	18 mm	13 mm
K50	24 mm	R	44 mm	34 mm	19 mm	26 mm	44 mm	40 mm	37 mm	26 mm	21 mm	24 mm	25 mm	39 mm	20 mm	40 mm	16 mm	13 mm
K17	24 mm	R	34 mm	26 mm	24 mm	24 mm	29 mm	29 mm	R	18 mm	R	12 mm	11 mm	27 mm	14 mm	23 mm	13 mm	9 mm
K45	24 mm	R	31 mm	19 mm	17 mm	25 mm	34 mm	29 mm	R	19 mm	16 mm	17 mm	14 mm	24 mm	14 mm	20 mm	14 mm	11 mm
K51	27 mm	R	42 mm	29 mm	23 mm	32 mm	39 mm	34 mm	R	25 mm	15 mm	20 mm	14 mm	40 mm	19 mm	39 mm	15 mm	11 mm
K5	39 mm	R	39 mm	26 mm	33 mm	20 mm	33 mm	30 mm	R	34 mm	22 mm	24 mm	27 mm	40 mm	14 mm	39 mm	17 mm	14 mm

Table 3 (continued)

	Ciprofloxacin	Sulfamethoxazole	Cefoperazone	Chloramphenicol	Ofloxacin	Vancomycin	Amoxicillin	Ampicillin	Sulbactam	Netilmicin	Streptomycin	Gentamicin	Kanamycin	CHX	PCQD	PCQDs@CHX	AgNPs@PCQD	AgNP
K47	36 mm	R	39 mm	39 mm	25 mm	27 mm	39 mm	34 mm	R	21 mm	19 mm	14 mm	13 mm	37 mm	16 mm	38 mm	14 mm	12 mm
K18	26 mm	R	39 mm	34 mm	23 mm	23 mm	36 mm	34 mm	R	17 mm	9 mm	16 mm	9 mm	34 mm	24 mm	34 mm	16 mm	14 mm

R resistant

damage caused by free radicals. In this study, the antioxidant activity of the synthesized AgNPs, PCQDs, and AgNPs@PCQDs was evaluated using DPPH and FRAP assays, with BHA and α-tocopherol serving as reference standards.

3.5.1 DPPH assay

DPPH is a stable radical with a characteristic purple color and is commonly used in antioxidant studies. Upon reaction with an antioxidant (as a hydrogen or electron donor), it is reduced, resulting in a color change from purple to yellow. In this study, two concentrations (30 and 50 µL/mL) of AgNPs, PCQDs, and AgNPs@PCQDs were prepared and measured at 517 nm using a spectrophotometer. All measurements were performed in triplicate, and mean values with standard deviations were calculated to ensure data accuracy.

As shown in Table 4, AgNPs exhibited approximately 35.1 ± 1.3% antioxidant activity at 30 µL/mL and 39.69 ± 0.9% at 50 µL/mL, consistent with previous reports [72, 73]. PCQDs demonstrated a markedly higher DPPH radical-scavenging activity, reducing DPPH radicals by about 93.4 ± 0.3% at both concentrations, in agreement with prior studies [74, 75]. Additionally, the DPPH radical scavenging activity of AgNPs@PCQDs was recorded as 60.6 ± 0.8% and 64.1 ± 1.1% at 30 µL/mL and 50 µL/mL, respectively.

The results confirm that antioxidant activity increases with concentration. However, a saturation trend is observed at higher concentrations, suggesting that the radical scavenging efficiency may plateau above 50 µL/mL.

3.5.2 FRAP assay

This assay is based on the ability of antioxidants to reduce Fe^{3+} to Fe^{2+}, which results in a color change from colorless to blue upon successful reduction. AgNPs, PCQDs, and AgNP@PCQDs were tested using this method at two concentrations (30 and 50 µL/mL). All samples were analyzed in triplicate, and mean values with standard deviations were calculated to ensure measurement accuracy.

As presented in Table 5, the reducing power of AgNPs, PCQDs, and AgNP@PCQDs increased with increasing concentration, indicating dose-dependent antioxidant behavior. AgNPs exhibited absorbance values of 0.31 ± 0.05 and 0.75 ± 0.03 at 30 and 50 µL/mL, respectively [76, 77]. The reducing power of PCQDs was determined as 0.49 ± 0.02 and 1.06 ± 0.04 at 30 and 50 µL/mL, respectively [75]. Furthermore, the AgNPs@PCQDs composite exhibited higher reducing power than AgNPs and was comparable to PCQDs, with values of 0.42 ± 0.06 and 0.87 ± 0.02 at 30 and 50 µL/mL, respectively.

Table 4 DPPH radical scavenging activity (%) of AgNPs, PCQDs, and AgNPs@PCQDs at different concentrations (mean ± SD, $n = 3$)

Treatment groups	% DPPH scavenging activity	
	30 µL/mL	50 µL/mL
AgNP	35.11 ± 1.3	39.69 ± 0.9
PCQD	93.37 ± 0.4	93.57 ± 0.4
AgNP/PCQD	60.58 ± 0.7	64.10 ± 1.1
BHA	66.49 ± 0.6	77.70 ± 0.8
α-Tocopherol	63.54 ± 0.8	74.13 ± 0.6

Table 5 FRAP activity (%) of AgNPs, PCQDs, and AgNPs@PCQDs at different concentrations (mean ± SD, $n = 3$)

Treatment groups	Ferrous Ion Chelating Activity	
	30 µL/mL	50 µL/mL
AgNP	0.31 ± 0.05	0.75 ± 0.03
PCQD	0.49 ± 0.02	1.06 ± 0.04
AgNP/PCQD	0.42 ± 0.06	0.87 ± 0.02
BHA	0.16 ± 0.01	0.19 ± 0.01
α-Tocopherol	0.12 ± 0.02	0.49 ± 0.05

For comparison, the standard antioxidants BHA and α-tocopherol exhibited lower reducing activities, with values of 0.16 ± 0.01 and 0.19 ± 0.01 for BHA and 0.12 ± 0.02 and 0.49 ± 0.05 for α-tocopherol at 30 and 50 µL/mL, respectively. These results clearly demonstrate that PCQDs and AgNPs@PCQDs have superior electron-donating ability compared to conventional antioxidants, consistent with literature reports [75–77].

4 Conclusion

Propolis was employed as a natural precursor for the synthesis of CQDs, which exhibited significant antibacterial activity. It is anticipated that PCQDs can exert antibacterial activity against pathogens responsible for periodontal abscesses under light stimulation and may serve as photosensitizers in photodynamic therapy, representing an alternative approach to conventional antibiotics. Furthermore, such comprehensive antibiotic testing is rarely reported in the literature. This study addressed which antibiotics bacteria causing dental abscesses are resistant or sensitive to, and whether the synthesized PCQDs and AgNPs possess antibacterial activity. If so, they could potentially serve as an alternative to standard antibiotics. The results indicated that PCQDs derived from propolis, a naturally abundant substance, demonstrate antibacterial activity against periodontal pathogens and may serve as a safe and effective alternative to standard antibiotics. Additionally, chlorhexidine, widely used in dental treatments, was found to enhance their activity. These findings suggest that such nanoparticles could potentially be incorporated into future toothpaste and mouthwash formulations.

Supplementary Information The online version contains supplementary material available at https://doi.org/10.1007/s43630-025-00842-4.

Acknowledgements We express our sincere gratitude to Prof. Dr. Özlem Barış for kindly providing us with bacterial strains for this research.

Author contributions Ruba Jebril: methodology, conceived and designed the analysis; performed the analysis; writing—original draft. Seyda Albayrak: methodology; performed the analysis, writing—original draft. Hayrunnisa Nadaroglu: methodology, conceptualization. Ahmet Adiguzel: methodology, conceptualization, writing—original draft, conceptualization.

Funding Open access funding provided by the Scientific and Technological Research Council of Türkiye (TÜBİTAK). The author(s) reported that there is no funding associated with the work featured in this article.

Data availability No datasets were generated or analysed during the current study.

Declarations

Conflict of interest The authors declare no competing interests.

Ethical approval This article does not involve any study with human participants or animals to be performed by any of the authors.

Consent to participate Not applicable.

Consent for publication All authors consent when it is submitted. Conflict of interest: The authors declare no competing interests.

Open Access This article is licensed under a Creative Commons Attribution 4.0 International License, which permits use, sharing, adaptation, distribution and reproduction in any medium or format, as long as you give appropriate credit to the original author(s) and the source, provide a link to the Creative Commons licence, and indicate if changes were made. The images or other third party material in this article are included in the article's Creative Commons licence, unless indicated otherwise in a credit line to the material. If material is not included in the article's Creative Commons licence and your intended use is not permitted by statutory regulation or exceeds the permitted use, you will need to obtain permission directly from the copyright holder. To view a copy of this licence, visit http://creativecommons.org/licenses/by/4.0/.

References

1. Karacam, K., Demir, T., & Baris, O. (2022). Identification of dominant bacteria isolated from periodontal abscesses. *J Adv Oral Res*, *13*(1), 91–96. https://doi.org/10.1177/23202068211050772
2. Prakash, S. K. (2013). Dental abscess: A Microbiological review. *Dental Research Journal*, *10*(5), 585.
3. Irshad, M., Alam, M. K., Alawneh, A., Alhadi, M. A., Alhadi, A. A., Almunajem, Y. S., & Kamal, M. A. (2020). Characterization and antimicrobial susceptibility of pathogens associated with

periodontal abscess. *Antibiotics*, *9*(10), 654. https://doi.org/10.3390/antibiotics9100654
4. Leroy, R., Bourgeois, J., Verleye, L., & Toma, S. (2022). Should systemic antibiotics be prescribed in periodontal abscesses and pericoronitis? A systematic review of the literature. *European Journal of Oral Sciences*, *130*(4), e12884. https://doi.org/10.1111/eos.12884
5. Herrera, D., Alonso, B., de Arriba, L., Santa Cruz, I., Serrano, C., & Sanz, M. (2014). Acute periodontal lesions. *Periodontology 2000*, *65*(1), 149–177. https://doi.org/10.1111/prd.12022
6. Radmila, O. R., Draginja, K. B., & Vesna, B. R. (2008). The therapy of periodontal abscess. *Acta Stomatologica Naissi*, 24(57).
7. Amato, A. (2023). Oral microbiota, bacterial infections, antibiotic prescriptions, and antimicrobial resistance in children. *Microorganisms*, *11*(8), 1927. https://doi.org/10.3390/microorganisms11081927
8. Michael, C. A., Dominey-Howes, D., & Labbate, M. (2014). The antimicrobial resistance crisis: causes, consequences, and management. *Frontiers in Public Health*, *2*, 145. https://doi.org/10.3389/fpubh.2014.00145
9. Ventola, C. L. (2015). The antibiotic resistance crisis: Part 1: Causes and threats. *Pharmacy and Therapeutics*, *40*(4), 277.
10. Rather, I. A., Kim, B. C., Bajpai, V. K., & Park, Y. H. (2017). Self-medication and antibiotic resistance: Crisis, current challenges, and prevention. *Saudi Journal of Biological Sciences*, *24*(4), 808–812. https://doi.org/10.1016/j.sjbs.2017.01.004
11. Mobarki, N., Almerabi, B., & Hattan, A. (2019). Antibiotic resistance crisis. *Int J Med Dev Ctries*, *40*(4), 561–564. https://doi.org/10.24911/IJMDC.51-1549060699
12. Das, C. A., Kumar, V. G., Dhas, T. S., Karthick, V., Govindaraju, K., Joselin, J. M., & Baalamurugan, J. (2020). Antibacterial activity of silver nanoparticles (biosynthesis): A short review on recent advances. *Biocatalysis and Agricultural Biotechnology*, *27*, 101593. https://doi.org/10.1016/j.bcab.2020.101593
13. Bruna, T., Maldonado-Bravo, F., Jara, P., & Caro, N. (2021). Silver nanoparticles and their antibacterial applications. *International Journal of Molecular Sciences*, *22*(13), 7202. https://doi.org/10.3390/ijms22137202
14. Kim, S. H., Lee, H. S., Ryu, D. S., Choi, S. J., & Lee, D. S. (2011). Antibacterial activity of silver-nanoparticles against Staphylococcus aureus and Escherichia coli. *Korean J Microbiol Biotechnol*, *39*(1), 77–85. https://www.researchgate.net/publication/265988418
15. Tang, S., & Zheng, J. (2018). Antibacterial activity of silver nanoparticles: Structural effects. *Advanced Healthcare Materials*, *7*(13), 1701503. https://doi.org/10.1002/adhm.201701503
16. Yan, H., Li, P., Wen, F., Xu, Q., Guo, Q., & Su, W. (2023). Green synthesis of carbon quantum Dots from plant turmeric holds promise as novel photosensitizer for in vitro photodynamic antimicrobial activity. *Journal of Materials Research and Technology*, *22*, 17–34. https://doi.org/10.1016/j.jmrt.2022.11.090
17. Nie, X., Jiang, C., Wu, S., Chen, W., Lv, P., Wang, Q., … Wei, Q. (2020). Carbon quantum dots: A bright future as photosensitizers for in vitro antibacterial photodynamic inactivation. *Journal of Photochemistry and Photobiology B: Biology*, *206*, 111864. https://doi.org/10.1016/j.jphotobiol.2020.111864.
18. Kovačova, M., Špitalská, E., Markovic, Z., & Špitálský, Z. (2020). Carbon quantum Dots as antibacterial photosensitizers and their polymer nanocomposite applications. *Particle & Particle Systems Characterization*, *37*(1), 1900348. https://doi.org/10.1002/ppsc.201900348
19. Molaei, M. J. (2019). Carbon quantum Dots and their biomedical and therapeutic applications: A review. *RSC Advances*, *9*(12), 6460–6481.
20. Das, R., Bandyopadhyay, R., & Pramanik, P. (2018). Carbon quantum Dots from natural resource: A review. *Materials Today Chemistry*, *8*, 96–109. https://doi.org/10.1016/j.mtchem.2018.03.003
21. Sarkar, S., Singh, A. K., & Kulkarni, A. R. (2024). In situ O2-releasing quantum Dot composites with enhanced radical scavenging behaviour, biosafety, and broadband UV shielding applications. *Materials Today Chemistry*, *39*, 102162. https://doi.org/10.1016/j.mtchem.2024.102162
22. Liu, T., Pang, Q., Mai, K., He, X., Xu, L., Zhou, F., & Liu, Y. (2022). Silver nanoparticle@ carbon quantum Dot composite as an antibacterial agent. *RSC Advances*, *12*(16), 9621–9627.
23. Alavi, M., Jabari, E., & Jabbari, E. (2021). Functionalized carbon-based nanomaterials and quantum Dots with antibacterial activity: A review. *Expert Review of Anti-infective Therapy*, *19*(1), 35–44. https://doi.org/10.1080/14787210.2020.1810569
24. Almuhayawi, M. S. (2020). Propolis as a novel antibacterial agent. *Saudi Journal of Biological Sciences*, *27*(11), 3079–3086. https://doi.org/10.1016/j.sjbs.2020.09.016
25. Santos, L. M., Fonseca, M. S., Sokolonski, A. R., Deegan, K. R., Araújo, R. P., Umsza-Guez,M. A., Machado, B. A. (2020). Propolis: types, composition, biological activities,and veterinary product patent prospecting. *Journal of the Science of Food and Agriculture*, *100*(4), 1369–1382. https://doi.org/10.1002/jsfa.10024.
26. Belmehdi, O., El Menyiy, N., Bouyahya, A., El Baaboua, A., El Omari, N., Gallo, M., & Abrini, J. (2023). Recent advances in the chemical composition and biological activities of propolis. *Food Reviews International*, *39*(9), 6078–6128. https://doi.org/10.1080/87559129.2022.2089164
27. Lotfy, M. (2006). Biological activity of bee propolis in health and disease. *Asian Pacific Journal of Cancer Prevention*, *7*(1), 22–31.
28. Stojanović, S. T., Najman, S. J., Popov, B. B., & Najman, S. S. (2020). Propolis: Chemical composition, biological and Pharmacological activity–a review. *Acta Medica Medianae*, *59*(2).
29. Hosseinpour-Nader, A., Karimi, N., & Ghafari, H. A. (2023). Ex-vivo effects of propolis quantum dots-nisin-nanoquercetin-mediated photodynamic therapy on Streptococcus mutans biofilms and white spot lesions. *Photodiagnosis and Photodynamic Therapy*, *41*, 103255. https://doi.org/10.1016/j.pdpdt.2022.103255
30. Cicek, S., Gungor, A. A., Adiguzel, A., & Nadaroglu, H. (2015). Biochemical evaluation and green synthesis of nano silver using peroxidase from euphorbia (Euphorbia amygdaloides) and its antibacterial activity. *Journal of Chemistry*, *2015*(1), 486948. https://doi.org/10.1155/2015/486948
31. Safardoust-Hojaghan, H., Salavati-Niasari, M., Amiri, O., Rashki, S., & Ashrafi, M. (2021). Green synthesis, characterization and antimicrobial activity of carbon quantum dots-decorated ZnO nanoparticles. *Ceramics International*, *47*(4), 5187–5197. https://doi.org/10.1016/j.ceramint.2020.10.097
32. Boli, E., Prinos, N., Louli, V., Pappa, G., Stamatis, H., Magoulas, K., & Voutsas, E. (2022). Recovery of bioactive extracts from Olive leaves using conventional and microwave-assisted extraction with classical and deep eutectic solvents. *Separations*, *9*(9), 255. https://doi.org/10.3390/separations9090255
33. Jasrotia, T., Chaudhary, S., Kaushik, A., Kumar, R., & Chaudhary, G. R. (2020). Green chemistry-assisted synthesis of biocompatible Ag, Cu, and Fe2O3 nanoparticles. *Materials Today Chemistry*, *15*, 100214. https://doi.org/10.1016/j.mtchem.2019.100214
34. Nadaroglu, H., Onem, H., & Alayli Gungor, A. (2017). Green synthesis of Ce2 O3 NPs and determination of its antioxidant activity. *IET Nanobiotechnology*, *11*(4), 411–419. https://doi.org/10.1049/iet-nbt.2016.0138
35. Zejli, H., El Amrani, B., Metouekel, A., Bousseraf, F. Z., Fitat, A., Taleb, M., & Abdellaoui, A. (2024). Comparative assessment of total phenolics content and in vitro antioxidant capacity variations of leaf extracts of Origanum grossii and thymus pallidus.

Moroccan Journal of Chemistry, *12*(1), J–Chem. https://doi.org/10.48317/IMIST.PRSM/morjchem-v12i1.41383
36. Shehata, M. G., Ahmad, F. T., Badr, A. N., Masry, S. H., & El-Sohaimy, S. A. (2020). Chemical analysis, antioxidant, cytotoxic and antimicrobial properties of propolis from different geographic regions. *Annals of Agricultural Sciences*, *65*(2), 209–217. https://doi.org/10.1016/j.aoas.2020.12.001
37. Bozkus, T. N., Deger, O., & Yasar, A. (2021). Chemical characterization of water and ethanolic extracts of Turkish propolis by HPLC-DAD and GC-MS. *Journal of Liquid Chromatography & Related Technologies*, *44*(1–2), 77–86. https://doi.org/10.1080/10826076.2021.1883648
38. Duran, N., Muz, M., Culha, G., Duran, G., & Ozer, B. (2011). GC-MS analysis and antileishmanial activities of two Turkish propolis types. *Parasitology Research*, *108*(1), 95–105. https://doi.org/10.1007/s00436-010-2039-z
39. Mohiuddin, I., Kumar, T. R., Zargar, M. I., Wani, S. U. D., Mahdi, W. A., Alshehri,S., … Shakeel, F. (2022). GC-MS analysis, phytochemical screening, and antibacterial activity of Cerana indica propolis from Kashmir region. *Separations*, *9*(11), 363. https://doi.org/10.3390/separations9110363.
40. Machado, C. S., Finger, D., Caetano, I. K., & Torres, Y. R. (2024). Multivariate GC-MS data analysis of the apolar fraction of brown propolis produced in Southern Brazil. *Journal of Apicultural Research*, *63*(5), 1038–1049. https://doi.org/10.1080/00218839.2023.2212487
41. Chowdhury, D., Majumdar, S., & Thakur, D. (2020). Actinobacteria mediated synthesis of bio-conjugate of carbon Dot with enhanced biological activity. *Applied Nanoscience*, *10*(7), 2199–2206. https://doi.org/10.1007/s13204-020-01392-0
42. Suriati, G., Mariatti, M., & Azizan, A. (2014). Synthesis of silver nanoparticles by chemical reduction method: Effect of reducing agent and surfactant concentration. *International journal of automotive and mechanical engineering*, *10*, 1920. https://doi.org/10.15282/ijame.10.2014.9.0160
43. Sholikhah, U., Pujiyanto, A., Lestari, E., Sarmini, E., & Lubis, H. (2018). Critical parameters of silver nanoparticles (AgNPs) synthesized by sodium borohydride reduction. *Res J Chem Environ 22 (Special Issue II) August (2018)*, *22(2)*, 179–183.
44. Guo, Y., & Zhao, W. (2020). Hydrothermal synthesis of highly fluorescent nitrogen-doped carbon quantum Dots with good biocompatibility and the application for sensing ellagic acid. *Spectrochimica Acta Part A: Molecular and Biomolecular Spectroscopy*, *240*, 118580. https://doi.org/10.1016/j.saa.2020.118580
45. Atchudan, R., Edison, T. N. J. I., Shanmugam, M., Perumal, S., Somanathan, T., & Lee, Y. R. (2021). Sustainable synthesis of carbon quantum Dots from banana Peel waste using hydrothermal process for in vivo bioimaging. *Physica E: Low-dimensional Systems and Nanostructures*, *126*, 114417. https://doi.org/10.1016/j.physe.2020.114417
46. Aslan, M., & Eskalen, H. (2021). A study of carbon nanodots (carbon quantum dots) synthesized from Tangerine juice using one-step hydrothermal method. *Fullerenes Nanotubes and Carbon nanostruCtures*, *29*(12), 1026–1033. https://doi.org/10.1080/1536383X.2021.1926452
47. Szczepanowicz, K., Stefanska, J., Socha, R. P., & Warszynski, P. (2010). Preparation of silver nanoparticles via chemical reduction and their antimicrobial activity. *Physicochem Probl Miner Process*, *45*(2010), 85–98.
48. Lee, S. M., Song, K. C., & Lee, B. S. (2010). Antibacterial activity of silver nanoparticles prepared by a chemical reduction method. *Korean Journal of Chemical Engineering*, *27*(2), 688–692. https://doi.org/10.1007/s11814-010-0067-0
49. Maribel, G. (2008). Synthesis of silver nanoparticles by chemical reduction method and their antibacterial activity.
50. Akkaya, S. N., Almansour, A., Omeroglu, M. A., Nadaroglu, H., & Adiguzel, A. (2025). Eco-friendly synthesis of silver nanoparticles using lignin peroxidase produced from Caldibacillus Thermoamylovorans and cultivated on waste walnut shell. *FEMS Microbiology Letters*, 372. https://doi.org/10.1093/femsle/fnaf036
51. Chakravarty, A., Ahmad, I., Singh, P., Sheikh, M. U. D., Aalam, G., Sagadevan, S., & Ikram, S. (2022). Green synthesis of silver nanoparticles using fruits extracts of syzygium cumini and their bioactivity. *Chemical Physics Letters*, *795*, 139493. https://doi.org/10.1016/j.cplett.2022.139493
52. Mindivan, F. E. R. D. A., & Goktas, M. (2023). The green synthesis of carbon quantum Dots (CQDs) and characterization of Polycaprolactone (PCL/CQDs) films. *Colloids and Surfaces A: Physicochemical and Engineering Aspects*, *677*, 132446. https://doi.org/10.1016/j.colsurfa.2023.132446
53. Rojas-Valencia, O. G., Regules-Carrasco, M., Hernández-Fuentes, J., Reza-San Germán, C. M., Estrada-Flores, M., & Villagarcía-Chávez, E. (2021). Synthesis of blue emissive carbon quantum Dots from hibiscus Sabdariffa flower: Surface functionalization analysis by FT-IR spectroscopy. *Materialia*, *19*, 101182. https://doi.org/10.1016/j.mtla.2021.101182
54. Singh, H., Bamrah, A., Khatri, M., & Bhardwaj, N. (2020). One-pot hydrothermal synthesis and characterization of carbon quantum Dots (CQDs). *Materials Today: Proceedings*, *28*, 1891–1894. https://doi.org/10.1016/j.matpr.2020.05.297
55. Gomes, M. F., Gomes, Y. F., Lopes-Moriyama, A., de Barros Neto, E. L., & de Souza, C. P. (2019). Design of carbon quantum Dots via hydrothermal carbonization synthesis from renewable precursors. *Biomass Conversion and Biorefinery*, *9*(4), 689–694. https://doi.org/10.1007/s13399-019-00387-4
56. Korkmaz, N. (2020). Bioreduction: The biological activity, characterization, and synthesis of silver nanoparticles. *Turkish Journal of Chemistry*, *44*(2), 325–334.
57. Thiruvengadam, V., & Bansod, A. V. (2020). Characterization of silver nanoparticles synthesized using chemical method and its antibacterial property. *Biointerface Res Appl Chem*, *10*(6), 7257–7264.
58. Roh, J., & Kim, K. R. (2018). Antimicrobial activity of Korean propolis extracts on oral pathogenic microorganisms. *Journal of Dental Hygiene Science*, *18*(1), 18–23. https://doi.org/10.17135/jdhs.2018.18.1.18
59. Waldner-Tomic, N. M., Vanni, R., Belibasakis, G. N., Thurnheer, T., Attin, T., & Schmidlin, P. R. (2014). The in vitro antimicrobial efficacy of propolis against four oral pathogens: A review. *Dentistry Journal*, *2*(2), 85–97. https://doi.org/10.3390/dj2030085
60. Kaur, J., Bhattu, M., Rawat, M., Varma, R. S., Acevedo, R., Shaban, M., … Singh,J. (2023). Facile synthesis of carbon quantum dot/silver nanocomposite and its antimicrobial,catalytic and sensing applications. *Environmental research*, *237*, 116919. https://doi.org/10.1016/j.envres.2023.116919.
61. Alzahrani, S. O., Al-Ghamdi, S. A., Alsahag, M., Alatawi, K., Alaysuy, O., Al-Ahmed, Z. A., & El-Metwaly, N. M. (2023). Nanosilver-doped carbon quantum Dots for industrialization of efficacious textiles with superior UV-resistance and antimicrobial performance. *Diamond and Related Materials*, *138*, 110249. https://doi.org/10.1016/j.diamond.2023.110249
62. Roy, A. K., Kim, S. M., Paoprasert, P., Park, S. Y., & In, I. (2015). Preparation of biocompatible and antibacterial carbon quantum Dots derived from resorcinol and formaldehyde spheres. *Rsc Advances*, *5*(40), 31677–31682.
63. Salleh, A., Naomi, R., Utami, N. D., Mohammad, A. W., Mahmoudi, E., Mustafa, N., & Fauzi, M. B. (2020). The potential of silver nanoparticles for antiviral and antibacterial applications: A mechanism of action. *Nanomaterials*, *10*(8), 1566. https://doi.org/10.3390/nano10081566

64. Wolny-Koładka, K. A., & Malina, D. K. (2017). Silver nanoparticles toxicity against airborne strains of Staphylococcus spp. *Journal of Environmental Science and Health Part A*, *52*(13), 1247–1256. https://doi.org/10.1080/10934529.2017.1356186
65. Thomas, R., Soumya, K. R., Mathew, J., & Radhakrishnan, E. K. (2015). Inhibitory effect of silver nanoparticle fabricated urinary catheter on colonization efficiency of coagulase negative Staphylococci. *Journal of Photochemistry and Photobiology B: Biology*, *149*, 68–77. https://doi.org/10.1016/j.jphotobiol.2015.04.034
66. Zorraquín-Peña, I., Cueva, C., González de Llano, D., Bartolomé, B., & Moreno-Arribas, M. V. (2020). Glutathione-stabilized silver nanoparticles: Antibacterial activity against periodontal bacteria, and cytotoxicity and inflammatory response in oral cells. *Biomedicines*, *8*(10), 375. https://doi.org/10.3390/biomedicines8100375
67. Cotton, G. C., Gee, C., Jude, A., Duncan, W. J., Abdelmoneim, D., & Coates, D. E. (2019). Efficacy and safety of alpha lipoic acid-capped silver nanoparticles for oral applications. *RSC Advances*, *9*(12), 6973–6985.
68. Kumar, N. I. R. M. A. L., Das, S. A., T. Y. A. J., E. E. T., Jyoti, A. N. U. P. A. M., & Kaushik, S. A. (2016). N. K. E. T. Synergistic effect of silver nanoparticles with doxycycline against Klebsiella pneumoniae. *Int. J. Pharm. Pharm. Sci*, *8*(7), 183–186.
69. Di Giulio, M., Di Bartolomeo, S., Di Campli, E., Sancilio, S., Marsich, E., Travan, A., & Cellini, L. (2013). The effect of a silver nanoparticle polysaccharide system on Streptococcal and saliva-derived biofilms. *International Journal of Molecular Sciences*, *14*(7), 13615–13625. https://doi.org/10.3390/ijms140713615
70. Lara, H. H., Ayala-Núnez, N. V., Turrent, I., L. D. C., & Rodríguez Padilla, C. (2010). Bactericidal effect of silver nanoparticles against multidrug-resistant bacteria. *World Journal of Microbiology and Biotechnology*, *26*(4), 615–621. https://doi.org/10.1007/s11274-009-0211-3
71. Chatzimitakos, T., & Stalikas, C. (2020). Antimicrobial properties of carbon quantum dots. In *Nanotoxicity* (pp. 301–315). Elsevier. https://doi.org/10.1016/B978-0-12-819943-5.00014-2
72. Kumari, S. A., Patlolla, A. K., & Madhusudhanachary, P. (2022). Biosynthesis of silver nanoparticles using Azadirachta indica and their antioxidant and anticancer effects in cell lines. *Micromachines*, *13*(9), 1416. https://doi.org/10.3390/mi13091416
73. Yadav, R., & Preet, S. (2023). Comparative assessment of green and chemically synthesized glutathione capped silver nanoparticles for antioxidant, mosquito larvicidal and eco-toxicological activities. *Scientific Reports*, *13*(1), 8152. https://doi.org/10.1038/s41598-023-35249-7
74. Kuppusamy, P., Kim, S., Park, M., & Song, K. D. (2024). Commercial wheat and oat flour derived fluorescent carbon quantum Dots through sustainable hydrothermal synthesis and their biological activities. *ChemistrySelect*, *9*(11), e202303994. https://doi.org/10.1002/slct.202303994
75. Wen, F., Li, P., Zhang, Y., Zhong, H., Yan, H., & Su, W. (2023). Preparation, characterization of green tea carbon quantum dots/curcumin antioxidant and antibacterial nanocomposites. *Journal of Molecular Structure*, *1273*, 134247. https://doi.org/10.1016/j.molstruc.2022.134247
76. Karan, T., Gonulalan, Z., Erenler, R., Kolemen, U., & Eminagaoglu, O. (2024). Green synthesis of silver nanoparticles using Sambucus Ebulus leaves extract: Characterization, quantitative analysis of bioactive molecules, antioxidant and antibacterial activities. *Journal of Molecular Structure*, *1296*, 136836. https://doi.org/10.1016/j.molstruc.2023.136836
77. Erenler, R., Gecer, E. N., Hosaflioglu, I., & Behcet, L. (2023). Green synthesis of silver nanoparticles using stachys spectabilis: Identification, catalytic degradation, and antioxidant activity. *Biochemical and Biophysical Research Communications*, *659*, 91–95. https://doi.org/10.1016/j.bbrc.2023.04.015